ACS EARTH AND SPACE CHEMISTRY

http://pubs.acs.org/journal/aesccq

Article

Autonomous Ion-Sensitive Field Effect Transistor-Based Total Alkalinity and pH Measurements on a Barrier Reef of Kāne'ohe Bay

Ellen M. Briggs, Eric Heinen De Carlo, Christopher L. Sabine, Noah M. Howins, and Todd R. Martz*

Cite This: *ACS Earth Space Chem.* 2020, 4, 355−362

Read Online

ACCESS | Metrics & More | Article Recommendations

ABSTRACT: Here, we present first of its kind high-frequency total alkalinity (A_T) and pH data from a single solid-state autonomous sensor collected during a six-day deployment at a barrier reef in Kāne'ohe Bay on the CRIMP-2 buoy. This dual parameter sensor is capable of rapid (<60 s), near-simultaneous measurement of the preferred seawater carbonate system parameters, pH, and A_T without requiring any external reagents or moving parts inherent to the sensor. Its solid-state construction, low power consumption, and low titrated volume (nanoliters) requirement make this sensor ideal for in situ monitoring of the aqueous carbon dioxide system. Through signal-averaging, we estimate the pH−A_T sensor is capable of achieving 2−10 μmol kg^{-1} precision in A_T and 0.005 for pH. The CRIMP-2 site in Hawai'i provided an excellent means of validation of the prototype pH−A_T sensor because of extensive observations routinely collected at this site and large daily fluctuations in A_T (∼116 μmol kg^{-1}) driven primarily by high calcification during the day and occasional $CaCO_3$ mineral dissolution at night. High-frequency sampling by the pH−A_T sensor reveals details in the diurnal cycle that are nearly impossible to observe by discrete sampling. Greater temporal resolution of the aqueous carbon dioxide system is essential for differentiating various drivers of coral reef health and the response to external influences such as ocean warming and acidification.

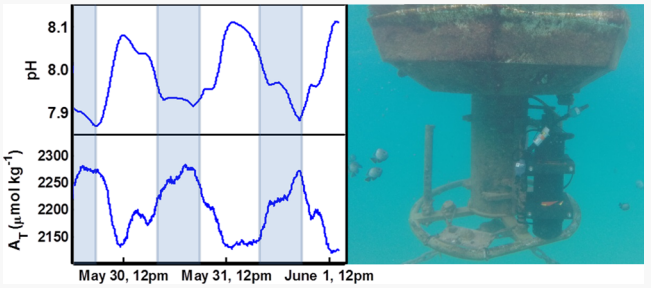

KEYWORDS: *total alkalinity, pH, high-frequency, calcification, autonomous, seawater*

INTRODUCTION

Tropical coral reefs are particularly vulnerable to global changes in sea surface temperature, ocean acidification, and rainfall patterns in addition to the local stresses induced by human activity around the reefs.[1−4] Coral reef ecosystems provide humanity with a range of direct (tourism, fishing), indirect (shoreline protection, fisheries recruitment), and non-use (biodiversity, intrinsic value) ecosystem services.[5] Therefore, it is essential to monitor the changing seawater conditions and the associated ecosystem responses, in order to understand the impacts of changing environmental conditions on these important economic resources.

Calcification rate and net ecosystem calcification (NEC), which is gross calcification minus dissolution, are indicators of coral reef health; however, we are limited in our ability to make direct in situ observations of the key parameters of the aqueous carbon dioxide system to estimate NEC because of the unavailability of commercial autonomous sensing technology. Discrete, laboratory-based measurements provide useful insight but are not always able to capture biogeochemical processes at relevant time scales necessary to decouple the range of highly correlated and interdependent interactions between environmental factors. Laboratory studies have examined the relationships between coral calcification rates and independently altered environmental parameters (e.g., temperature, light, pH, and saturation state); however, relatively few studies have explored the combined effects under naturally variable in situ conditions.[2,3,6−11]

It is hypothesized that calcification rates vary over a range of time scales from hours to seasons based on different drivers.[12−14] On shorter time scales, calcification is driven by local, short-term variations in biology and saturation state driven by diurnal variations in light, local heating, and the ratio of productivity to respiration. Over longer time scales, weeks to seasons, variations in calcification are driven by changes in local biological processes, as well as variations in the properties of seawater crossing the reef. Our ability to resolve the relative importance of different drivers of calcification in the field is limited by the inability to accurately measure, simultaneously and autonomously, chemical properties at relevant timescales. To achieve this, automated sampling systems or autonomous sensors with high sampling frequency capabilities are needed.

Received: October 14, 2019
Revised: January 3, 2020
Accepted: February 7, 2020
Published: February 7, 2020

Autosamplers have been deployed in coral reef studies[9] in order to provide higher frequency data sets (~1 sample every 2 h) than are possible by manual collection of discrete samples; however, the limited number of sample bottles and subsequent benchtop bottle analysis time (~5−30 min per sample) typically limit the utility of autosamplers for long-term, higher-frequency monitoring.

The four measurable CO_2 system variables are pH, partial pressure of carbon dioxide (pCO_2), total dissolved inorganic carbon ($C_T = [CO_2]_{aq} + [H_2CO_3] + [HCO_3^-] + [CO_3^{2-}]$), and total alkalinity (A_T = proton acceptors−proton donors ≈ $2[CO_3^{2-}] + [HCO_3^-] + [OH^-] - [H^+]$). Although commercial autonomous sensors are available for pCO_2 and pH, their strong covariance makes this measurement combination the least desirable for distinguishing between the biological processes described above. Because two system variables must be known to fully constrain the inorganic carbon system and because A_T is the seawater parameter that most directly reflects changes due to calcification, the pH−A_T or pCO_2−A_T pairs are most suitable for coral reef studies.[15] Traditional approaches to the determination of A_T require an acid−base titration[16] that is difficult to automate into a robust field-based sensor because of instrument complexity, inability to miniaturize, power consumption, and need for reagents. Several emerging (prototype stage) technologies for automated/autonomous measurement of seawater A_T have been reported, including chronopotentiometry,[17−19] single-point titration with spectrophotometric detection,[20] and tracer monitored titrations.[21,22] Each of these approaches offers a unique set of advantages and limitations, depending on the type of field applications. These prototype-level technologies, however, are currently not commercially available to the community. Another challenge with these systems is they only address one of the two carbon variables required to fully constrain the aqueous carbon dioxide system, necessitating additional instrumentation that might not be suitable or possible for all platforms with limited payload capacity such as profiling floats or gliders. Additionally, mismatch in timing between two separate sensors can lead to large errors in computing the aqueous carbon dioxide system.[15]

Here, we report the first field data from the deployment of a prototype autonomous, dual pH−A_T sensor,[23] utilizing solid-state ion-sensitive field effect transistor (ISFET) technology on the Coral Reef Instrumented Monitoring Platform (CRIMP-2) buoy in Kāne'ohe Bay, O'ahu, HI. We demonstrate that this dual parameter sensor is capable of rapid (<60 s), near-simultaneous measurement of the preferred carbonate system parameters, pH and A_T, without requiring any external reagents or moving parts inherent to the sensor, although a submersible pump is used to flush the sample in a manner analogous to a common CTD (conductivity, temperature, and depth instrument) configuration. The solid-state construction, near-zero sample consumption (nanoliters), and low power consumption make this sensor ideal for in situ monitoring of the aqueous carbon dioxide system. Preliminary results indicate an achievable precision of 2−10 μmol kg^{-1} for A_T and 0.005 for pH, which allows a number of immediate applications for studying marine biogeochemical processes and indicate that the sensor could be a valuable tool for the coral reef community and ocean acidification research.

ISFET pH-sensing technology is in widespread use throughout the field of oceanography on a variety of platforms ranging from moorings to profiling floats.[24−26] The dual pH−A_T sensor is uniquely capable of being easily mounted on a variety of platforms or placed very close to substrates to acquire near-field measurements that are difficult to obtain otherwise. This sensor has potential applications not only in studying coral reef ecosystems in situ but also in porewater studies,[27] open ocean monitoring during calcification events such as coccolithophore blooms, and other regions where non-conservative behavior in A_T is known to occur.[28−30]

METHODS: PH−A_T SENSOR PACKAGE

The autonomous sensor package (Figure 1) is based on modifications to the SeapHOx design.[26] The SeapHOx

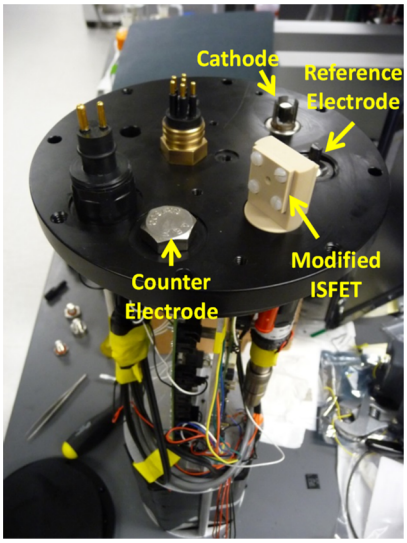

Figure 1. Top end-cap view of the modified ISFET, reference electrode, counter electrode, and cathode while enclosing microcontroller and batteries.

configuration integrates a Honeywell Durafet ISFET sensor to measure pH on the total hydrogen ion scale (pH_{tot}), Aanderaa optode (AADI 3835) to measure dissolved oxygen, and a Sea-Bird conductivity-temperature sensor (SBE-37) to measure salinity. In the prototype tested in this work, the oxygen sensor was removed and replaced with the custom-modified ISFET sensor which measures both pH and A_T. The commercial Durafet sensor (a combination electrode) remained installed during the deployment but was only used as a reference electrode half cell for the pH−A_T sensor (i.e., the ISFET of the commercial Durafet was disconnected).[23] In the pH mode, the ISFET sensor is operated in its normal state.[31] In the A_T mode, the titrant, H^+, is generated through the electrolysis of water by applying an anodic current pulse to an actuator electrode with respect to a cathodic electrode in solution. A nL-scale acid−base titration can then be performed by placing the actuator electrode on the surface of the ISFET near the ion-sensing region of the chip so that the pH can be rapidly measured as the analyte solution is titrated with the electrolytically generated H^+. We refer to the technique used in the ISFET-based coulometric sensor-actuator system as a coulometric diffusion titration which can be described by a one-dimensional diffusive mass transport model.[32]

The ISFET was modified by adding a Pt anode (actuator electrode) approximately 100 μm from the ion-sensing region of the chip and was then encapsulated following the methods described in Briggs et al.[23] The SeapHOx microcontroller

https://dx.doi.org/10.1021/acsearthspacechem.9b00274
ACS Earth Space Chem. 2020, 4, 355−362

(based on an ARM TI Cortex TM4C123G) was also modified in order to perform the A_T measurement. All of the sensor components (modified ISFET, reference electrode, counter electrode, and cathode, shown in Figure 1) are enclosed within a pumped flow cell using a SeaBird submersible pump (SBE 5M). The internal Ag/AgCl reference electrode of a Honeywell Durafet III pH sensor was used as the reference electrode. A simple seal screw was used as the ISFET counter electrode, which serves as a pseudogate and is used for controlling the operating current and voltage of the ISFET while providing a low impedance pathway for parasitic leakage currents.[33] The Pt half-cell of an Orion ORP combination electrode was used as the electrolysis cathode.

A series of four swing check valves (Spears S1520C05F) was configured as shown in Figure 2 to restrict flow through the

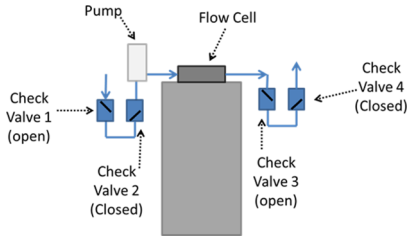

Figure 2. Diagram of the check valve configuration for the pH–A_T sensor which significantly reduced turbulence within the flow cell caused by wave motion during the titration when it is critical for the sample solution to remain static.

flow cell until the pump was turned on between measurements. This critical component of the design blocks flow during the titration when it is necessary to eliminate all turbulence in the sensor caused by buoy motion and water flow around the sensor package for the diffusion-based A_T measurement. When the buoy is stable and turbulent seawater flows against the sensor package, check valves 2 and 4 are closed and check valves 1 and 3 remain open. When the buoy and sensor package move downward, check valves 1 and 3 are force-closed while check valves 2 and 4 are allowed to open. When the buoy and sensor package move upward, check valves 2 and 4 are force-closed and check valves 1 and 3 remain open. Horizontal movement and flow are blocked by check valves 2 and 4 when they are oriented in the vertical direction. The appropriate swing valves were selected that would open under the force of the submersible pump to refresh the sensor surface between titrations.

METHODS: FIELD DEPLOYMENT

The pH–A_T sensor was deployed in Kāne'ohe Bay at ~1 m depth on the CRIMP-2 pCO_2 buoy (see Figure 3), which is part of a network of coastal MAPCO$_2$ buoys (moored pCO_2 systems).[34] Kāne'ohe Bay, located on the eastern side of O'ahu, Hawai'i, is the largest sheltered body of water in the Hawaiian Islands and is made up of a complex estuarine system with a large barrier coral reef (~10 km long by 2 km wide), patch reefs, fringing reefs, and multiple riverine inputs (Figure 3).[35] Water generally flows from the open ocean over the barrier reef into the lagoon and out through two deep channels in the northern and central bay. Circulation in the bay is driven primarily by wave action across the barrier reef crest with the additional effects of wind and tides. Water residence time

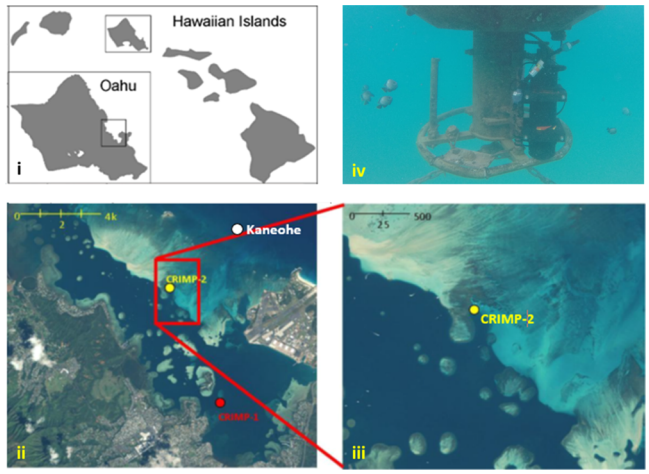

Figure 3. Map of buoy locations on northeastern shore of O'ahu, HI (panels i,ii). CRIMP-2 is the location of the deployment site of the pH–A_T sensor, as shown in panel (iii). The pH–A_T sensor was secured to the CRIMP-2 buoy at about 1 m depth (panel iv).

ranges from one day or less on the barrier reef flat and up to a month or more in the restricted southern bay.[36−38]

Four MAPCO$_2$ buoy sites, with a variety of autonomous instruments as well as regular discrete validation measurements, are located around O'ahu, providing an opportunity to test new instrumentation (sensors) and techniques for studying ocean acidification under a variety of conditions. CRIMP-2 is located on the inner edge of the Kāne'ohe Bay barrier reef in about 3 m seawater over sandy benthos and measures surface water and atmospheric pCO_2 in addition to temperature, salinity, dissolved oxygen, turbidity, and chl-*a* fluorescence every 3 h. CRIMP-2 has often been used as a platform for evaluation of prototype autonomous sensors designed primarily for ocean acidification research,[22,39] as well as for field evaluation of commercially available sensors (e.g., both pCO_2 analyzers and pH sensors).[40] The CRIMP-2 site was specifically chosen for this study because of the occurrence of large diurnal fluctuations in A_T in the water column primarily driven by high calcification during the day and occasional $CaCO_3$ mineral dissolution at night.[9] The porewater of carbonate sediments around O'ahu, Hawai'i, including the CRIMP-2 site, is also subject to a wide range in A_T in response to both changing conditions in the overlying water column and organic matter remineralization in the sediments, which leads to dissolution of high magnesian calcites.[41,42]

The pH–A_T sensor underwent two preliminary test deployments on the CRIMP-2 buoy in mid-December 2017 to early-January 2018. Data from these initial tests are not discussed here, yet the deployments are noteworthy because they served to identify critical design shortcomings, leading to modifications designed to reduce internal flow cell volume (from ~200 to ~100 mL) and, most importantly, develop a working check valve configuration to minimize turbulence in the cell. The third deployment, discussed here, took place from May 26, 2018 through June 1, 2018. The sensor was set to measure a pH and A_T value every 2 min. During each measurement cycle, the actuator current for generating the titrant is first turned off for 10 readings, recorded at 40 Hz, which are averaged to yield one pH measurement, and then, the anodic actuator current is turned on for the remaining ~80 s of the measurement cycle to carry out the A_T titration. Note

https://dx.doi.org/10.1021/acsearthspacechem.9b00274
ACS Earth Space Chem. 2020, 4, 355−362

the time required to reach the endpoint is ~20−30 s; however, the current is programmed to remain turned on except when the pump is running (10−20 s) at the start of the next measurement and during the collection of initial pH data (<1 s). This is done to maintain the surface chemistry of the anode and to improve the stability of proton generation between titrations.[23]

The individual titration curves were smoothed with a low pass filter before using a simple graphical analysis to determine the equivalence point.[23] The time required to reach the endpoint was converted to A_T using a linear calibration for the sensor (slope = 0.0039 s per μmol kg^{-1} A_T, intercept = 3.53) that was previously measured using seawater samples with known A_T ranging from 2217 to 2367 ($\pm$1.5) μmol kg^{-1} determined using standard benchtop analysis.[43] The resulting A_T time series (2 min resolution), shown in the bottom panel of Figure 4, was smoothed using a moving average with a window of 60 points in order to improve the signal to noise without compromising sensor resolution.

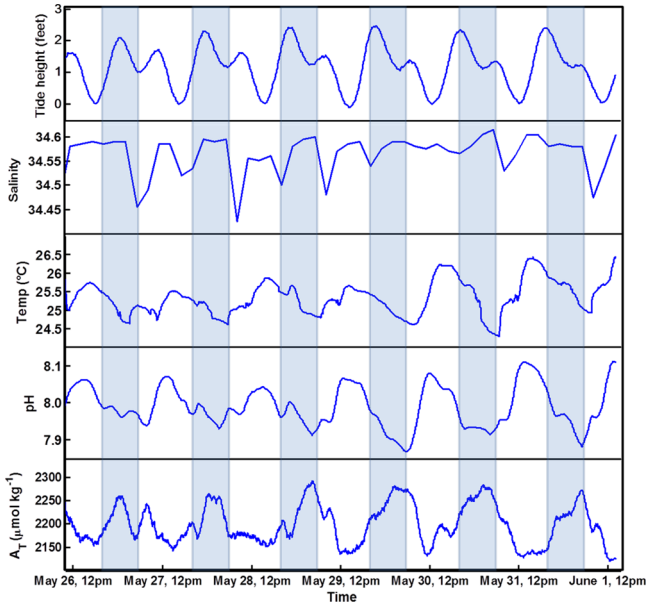

Figure 4. Tidal height data from Moku o Lo'e (Coconut Island, HI), temperature and salinity from the CRIMP-2 buoy, and pH and A_T from the pH−A_T autonomous sensor at CRIMP-2 buoy from May 26, 2018 to June 1, 2018. White bars indicate daylight (sunrise to sunset) and shaded bars indicate night. There is a large diurnal signal in A_T and pH indicative of alternating production/respiration and calcification/dissolution signals on the reef.

It is customary to apply final adjustments to Durafet pH sensor data based on either co-located bottle samples, historical data, or pH inferred from a combination of colocated biogeochemical sensors and empirical relationships used to derive an estimate of pH.[26,44] In this work, the final data quality control step was to adjust the mean pH observed by the sensor to fit the annual mean pH_{tot}, 7.96, observed in the historical bottle data samples at the CRIMP-2 (data available at: https://www.nodc.noaa.gov/ocads/oceans/Moorings/CRIMP2.html). As discussed below, based on the colocated and independent pCO_2 sensor, this adjustment led to a pH error of less than 0.01. The other carbonate variables were then derived from pH and A_T using the CO2SYS program.[45]

RESULTS AND DISCUSSION

The full sensor time series of A_T, pH, temperature, salinity, and tidal data are shown in Figure 4 and the other derived carbonate parameters are shown in Figure 5 for the 6 day

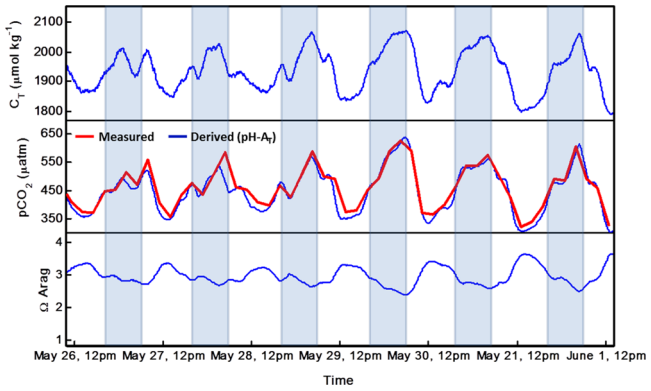

Figure 5. C_T, pCO_2 (blue), and Ω_{Arag}, aragonite saturation state, derived from the pH−A_T autonomous sensor at CRIMP-2 buoy from May 26, 2018 to June 1, 2018. White bars indicate daylight (sunrise to sunset) and shaded bars indicate night. For comparison, the seawater pCO_2 measured by the CRIMP-2 buoy is overlaid in red. There is very good agreement in the daily fluctuation of pCO_2 from the direct measurement and derived from the pH−A_T sensor with a mean percentage error of 2%.

deployment of the pH−A_T sensor at CRIMP-2 buoy in late May 2018. We observed, on average, a diurnal amplitude of 0.16 in pH_{tot}, with a range from 7.87 to 8.11 and a diurnal amplitude of 116 μmol kg^{-1} in A_T, with a range from 2121 to 2263 μmol kg^{-1} and mean value of 2199 μmol kg^{-1}. Because of logistical constraints, it was not possible to collect bottle samples at the CRIMP-2 site during this six-day deployment. Luckily, the large number of historical bottle samples collected at this site (see Table 1) makes it relatively straightforward to bracket an expected range and mean of seawater A_T and other measured and derived values. The bottle samples used to compute the statistics in Table 1 were sparsely collected over the time period of January 2016−May 2018 as a means of sensor validation at the CRIMP-2 buoy but are biased toward the morning hours and thus do not reflect the entire range of diurnal variability in the aqueous carbon dioxide system. However, Shamberger et al.[9] reported a drawdown in A_T of up to approximately 100 μmol kg^{-1} over a diurnal cycle at the CRIMP-2 site in response to day/night calcification/dissolution.

The other carbonate variables derived from pH and A_T, shown in Figure 5, also agree well with long-term observations at the CRIMP-2 site. The derived pCO_2 from the pH−A_T sensor output is compared to the measured pCO_2 by the CRIMP-2 buoy in Figure 5 (middle panel). There is excellent agreement in the daily pCO_2 range and the shape of the diurnal variations. The mean percentage error between the measured and derived pCO_2 is estimated to be ~2%. The mean derived C_T (total dissolved inorganic carbon) is 1941 μmol kg^{-1} compared to a mean annual C_T observed at CRIMP-2 from bottle samples of 1947 μmol kg^{-1}. The mean Ω_{Arag} over the six-day deployment was 2.95, which agrees well with the observed mean annual Ω_{Arag} of 2.85−2.92 at CRIMP-2 buoy from other studies.[9−11,46]

https://dx.doi.org/10.1021/acsearthspacechem.9b00274
ACS Earth Space Chem. 2020, 4, 355−362

Table 1. Statistics of the Seawater pCO_2, A_T, C_T, and pH at CRIMP-2 for January 2016−May 2018[a]

	min	max	mean	range	number of samples
pCO_2 sw (μatm)	258.3	823.0	488.0 ± 118.1	564.8	32
A_T (μmol kg^{-1})	2059.8	2268.9	2189.4 ± 42.2	209.1	53
C_T (μmol kg^{-1})	1832.3	2179.9	1947.2 ± 62.1	347.7	42
pH_{tot}	7.75	8.18	7.96 ± 0.09	0.43	32

[a]Parameter statistics were calculated from A_T and C_T validation bottle samples and available temperature and salinity data at CRIMP-2. Data are available at: https://www.nodc.noaa.gov/ocads/oceans/Moorings/CRIMP2.html.

As another check on the utility of the sensor, a simplified NEC, or gross calcification minus dissolution, calculation was made following Shamberger et al.[9] using eq 1 where ΔA_T is the daily amplitude in A_T calculated from the daily minimum to maximum of the smoothed signal, h is the average depth on the barrier reef (2 m), ρ is the density of seawater (kg m^{-3}), and $\Delta\tau$ is the mean residence time of 6.4 h estimated for the barrier reef (taken from Shamberger et al.[9])

$$\mathrm{NEC} = \Delta A_T h\rho/(2\Delta\tau) \quad (1)$$

From the daily A_T amplitude measured with this sensor, the NEC is estimated to range from 10.3 to 17.3 mmol $CaCO_3$ m^{-2} h^{-1}, which agrees well with prior studies at the CRIMP-2 site and fits well within the range of other strongly calcifying ecosystems. Although the NEC estimated from the pH−A_T sensor is slightly greater than the range of 7.3−13.8 mmol $CaCO_3$ m^{-2} h^{-1} reported by Shamberger et al.[9] and 4.2−12.8 mmol $CaCO_3$ m^{-2} h^{-1} by Courtney et al.,[10] it is less than the rates of up to 24.62 mmol $CaCO_3$ m^{-2} h^{-1} reported by Kealoha et al.[47] when flow was faster. Of course, the experiment presented here was not designed to assess NEC and assumes many of the same conditions of flow and initial A_T as Shamberger et al.,[9] but the estimate does demonstrate the value of having simultaneous rapid measurements of pH and A_T on a coral reef mooring.

It is important to note that the frequency of pCO_2 measurements made by the CRIMP-2 buoy is 3 h compared to the possible <60 s resolution of the autonomous pH−A_T sensor. Even with data smoothing, there are features that can be resolved on much shorter timescales by the pH−A_T sensor than is possible by discrete sampling or calculated from available in situ pH and pCO_2 sensors. The complexity of the autosampler instrumentation and the storage of samples in bags used by Shamberger et al.[9] and the total number of samples collected and analyzed in the recent work by Courtney et al.[10] study at the CRIMP-2 site have limitations and cannot be applied in many study sites, especially in remote locations or on moving platforms and numerous hours of laboratory analysis time are still required. The CRIMP-2 site is well studied and it is fairly simple to estimate the timing of the daily minimum and maximum A_T occurrences which is ideal for performing preliminary field testing and validation of the autonomous pH−A_T sensor. Most other reef ecosystems are neither as well studied nor nearly as predictable especially under changing environmental conditions. Thus, the technology demonstrated here has significant advantages over the traditional autosampler approach to calcification studies in remote locations.

As noted above, turbulence within the flow cell was recognized as a critical issue during a preliminary (December−January) deployment on the CRIMP-2 buoy because, in addition to turbulence of water around the sensor, the motion of the buoy and sensor also induced turbulence within the flow cell. During calmer periods, the preliminary deployment data did reveal a meaningful signal, although extensive processing and quality assessment were necessary to identify the periods that were not detrimentally impacted by turbulence. This led to the development and testing of alternative check valve configurations, leading to significant reduction in the turbulence issue within the flow cell and the very clear diurnal signal in A_T shown in Figure 4. In future iterations of the housing design, a single mechanical check valve could potentially replace the four swing check valve configuration to streamline the package. Alternatively, a small volume flow cell designed to encapsulate only the modified ISFET could aid in reducing turbulence at the ISFET surface without requiring the addition of moving parts.

Depending on the desired accuracy, frequency, and length of deployment, the sampling rate can be adjusted. The anode-gate distance of the sensor can also be modified to capture a narrower range of A_T at higher precision through sample averaging or larger range of A_T at the cost of increased measurement time. In the present configuration, the standard deviation over five data points averaged over the smoothed (60 point moving average) six-day time series was 1.9 μmol kg^{-1}. Because A_T naturally fluctuates over time, the standard deviation of multiple measurements taken over any time period is not entirely representative of sensor precision. This would be particularly true during times of rapidly changing A_T.

The precision of the Durafet pH sensor has been thoroughly evaluated and found to be better than 0.005 over long periods.[26] In order to assess A_T sensor precision, the A_T response was evaluated under stable conditions in a 5000 L test tank filled with seawater from the Scripps Pier (La Jolla, California). A_T was increased by two increments of approximately 50 μmol kg^{-1} by adding a concentrated solution of CO_3^{2-}, HCO_3^-, and NaCl in DI water. Bottle samples were taken at each A_T adjustment. A total of 800 measurements were collected by the pH−A_T sensor over the course of approximately 24 h after allowing the tank to completely mix after each A_T adjustment. The sensor precision is shown in Table 2 for six different averaging windows ranging from 0 to 60 samples. The approximate time required to collect a single

Table 2. Sensor A_T Precision for Raw and Averaged Data and the Minimum Time Required to Collect a Single Averaged Data Point

measurements averaged	A_T STD (μmol kg^{-1})	elapsed time (min)
none	15.9	<1
2	11.7	<2
10	4.7	7
20	3.3	13
30	2.7	20
60	1.9	40

https://dx.doi.org/10.1021/acsearthspacechem.9b00274
ACS Earth Space Chem. 2020, 4, 355−362

measurement is 40 s, reflecting 30 s titration and 10 s pump ON time. The measured A_T (benchtop) of the test tank was 2278.72, 2322.81, and 2366.11 μmol kg^{-1} and the mean A_T (sensor) using raw data was 2278 (n = 580), 2324 (n = 111), and 2366 (n = 109) μmol kg^{-1}, resulting in a root-mean-square error of 0.8 μmol kg^{-1}. Figure 6 shows sensor A_T minus measured A_T (benchtop) of the tank after averaging 2−60 points compared to the raw signal.

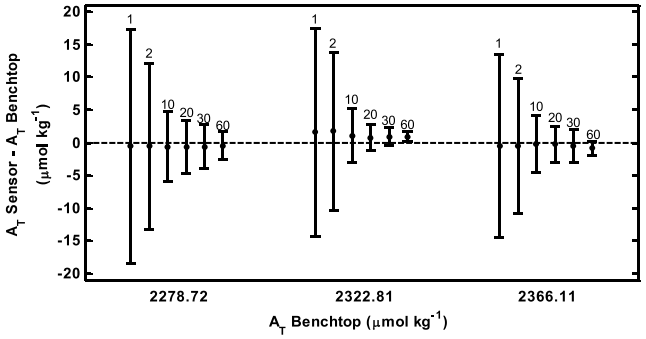

Figure 6. A_T data from the pH−A_T sensor deployed in a 5k L test tank filled with seawater from Scripps Pier over a 24 h period with 2 adjustments to the A_T verified by standard benchtop analysis. Sensor A_T minus measured A_T (benchtop) of the tank after averaging 2−60 points compared to the raw signal. Signal-averaging leads to a significant improvement in sensor precision.

Sensor encapsulation is one of the leading challenges in fabricating a successful sensor package that can withstand repeat deployments in corrosive environments. The pH−A_T sensor described here has shown a continuous wetted lifetime of several months during benchtop testing and overall wetted lifetime of more than one year for cumulative testing in the laboratory and field. The deployment endurance of the sensor is limited by power and depends on the operating frequency and pump time. The sampling rate of the sensor can be reduced in order to achieve longer-term observations and lower frequency time series. Because of the small footprint of the nL-scale acid−base titration measurement, there are numerous possibilities in the housing design to integrate this technology onto a variety of platforms including fixed moorings (as demonstrated in this study), as well as mobile platforms that demand high frequency measurements such as gliders and profiling floats. There are ongoing efforts to fine-tune and optimize the pH−A_T sensor over a range of temperature, salinity, and eventually pressure. Calibration protocols are already in place for temperature and pressure cycling of the ISFET pH sensor for profiling float applications.[24] Additional efforts will be required to assess proton evolution efficiency during the A_T measurement under varied environmental conditions (T, S, P). This ISFET-based pH−A_T sensor shows great potential for in situ observations on a variety of platforms providing high-frequency and long-term monitoring of the seawater carbon dioxide system and will be of great value, particularly for coral reef health monitoring and ocean acidification research.

AUTHOR INFORMATION

Corresponding Author

Todd R. Martz − *Scripps Institution of Oceanography, University of California San Diego, San Diego, California 92093, United States*; Phone: 858-534-7466; Email: trmartz@ucsd.edu

Authors

Ellen M. Briggs − *Scripps Institution of Oceanography, University of California San Diego, San Diego, California 92093, United States*; orcid.org/0000-0003-0202-8624

Eric Heinen De Carlo − *Department of Oceanography, University of Hawai'i at Mānoa, Honolulu, Hawaii 96822, United States*

Christopher L. Sabine − *Department of Oceanography, University of Hawai'i at Mānoa, Honolulu, Hawaii 96822, United States*

Noah M. Howins − *Department of Oceanography, University of Hawai'i at Mānoa, Honolulu, Hawaii 96822, United States*

Complete contact information is available at: https://pubs.acs.org/10.1021/acsearthspacechem.9b00274

Author Contributions

The manuscript was written through contributions of all authors. All authors have given approval to the final version of the manuscript.

Funding

This work was supported by grant NSF OCE Award 1155122 to T.R.M. The operation of the CRIMP-2 buoy is supported by a grant/cooperative agreement from the National Oceanic and Atmospheric Administration, Project I/IR-27, which is sponsored by the University of Hawai'i Sea Grant College Program, SOEST, under Institutional grant no. NA18OAR4170076 from NOAA Office of Sea Grant, Department of Commerce. The views expressed herein are those of the author(s) and do not necessarily reflect the views of NOAA or any of its subagencies.

Notes

The authors declare no competing financial interest.

ACKNOWLEDGMENTS

We would like to acknowledge the PMEL MAPCO$_2$ team (Sylvia Musielewicz, Stacy Maenner and Randy Bott) for buoy technical support and processing the pCO_2 data presented here. We would also like to thank the Hawai'i Institute of Marine Biology for access to small boats. This is SOEST contribution 10904 and Sea Grant contribution number UNIHI-SEAGRANT-JC-18-12.

REFERENCES

(1) Castillo, K. D.; Ries, J. B.; Bruno, J. F.; Westfield, I. T. The reef-building coral Siderastrea siderea exhibits parabolic responses to ocean acidification and warming. *Proc. R. Soc. B* **2014**, *281*, 20141856.

(2) Venti, A.; Andersson, A.; Langdon, C. Multiple driving factors explain spatial and temporal variability in coral calcification rates on the Bermuda platform. *Coral Reefs* **2014**, *33*, 979−997.

(3) Lough, J. M.; Cantin, N. E.; Benthuysen, J. A.; Cooper, T. F. Environmental drivers of growth in massive Porites corals over 16 degrees of latitude along Australia's northwest shelf. *Limnol. Oceanogr.* **2016**, *61*, 684−700.

(4) Yeakel, K. L.; Andersson, A. J.; Bates, N. R.; Noyes, T. J.; Collins, A.; Garley, R. Shifts in coral reef biogeochemistry and resulting acidification linked to offshore productivity. *Proc. Natl. Acad. Sci. U.S.A.* **2015**, *112*, 14512−14517.

(5) Spurgeon, J. P. G. The economic valuation of coral reefs. *Mar. Pollut. Bull.* **1992**, *24*, 529−536.

(6) Pratchett, M.; Anderson, K.; Hoogenboom, M.; Widman, E.; Baird, A.; Pandolfi, J.; Edmunds, P.; Lough, J. Spatial, temporal and

taxonomic variation in coral growth—implications for the structure and function of coral reef ecosystems. *Oceanogr. Mar. Biol.* **2015**, *53*, 215−296.
(7) McMahon, A.; Santos, I. R.; Cyronak, T.; Eyre, B. D. Hysteresis between coral reef calcification and the seawater aragonite saturation state. *Geophys. Res. Lett.* **2013**, *40*, 4675−4679.
(8) Massaro, R. F. S.; De Carlo, E. H.; Drupp, P. S.; Mackenzie, F. T.; Jones, S. M.; Shamberger, K. E.; Sabine, C. L.; Feely, R. A. Multiple Factors driving Variability of CO_2 Exchange Between the Ocean and Atmosphere in a Tropical Coral Reef Environment. *Aquat. Geochem.* **2012**, *18*, 357−386.
(9) Shamberger, K. E. F.; Feely, R. A.; Sabine, C. L.; Atkinson, M. J.; DeCarlo, E. H.; Mackenzie, F. T.; Drupp, P. S.; Butterfield, D. A. Calcification and organic production on a Hawaiian coral reef. *Mar. Chem.* **2011**, *127*, 64−75.
(10) Courtney, T. A.; De Carlo, E. H.; Page, H. N.; Bahr, K. D.; Barro, A.; Howins, N.; Tabata, R.; Terlouw, G.; Rodgers, K. S.; Andersson, A. J. Recovery of reef-scale calcification following a bleaching event in Kāne'ohe Bay, Hawai'i. *Limnol. Oceanogr. Lett.* **2018**, *3*, 1−9.
(11) Page, H. N.; Courtney, T. A.; De Carlo, E. H.; Howins, N. M.; Koester, I.; Andersson, A. J. Spatiotemporal variability in seawater carbon chemistry for a coral reef flat in Kāne'ohe Bay, Hawai'i. *Limnol. Oceanogr.* **2019**, *64*, 913−934.
(12) Bates, N. R.; Amat, A.; Andersson, A. J. Feedbacks and responses of coral calcification on the Bermuda reef system to seasonal changes in biological processes and ocean acidification. *Biogeosciences* **2010**, *7*, 2509−2530.
(13) Falter, J. L.; Lowe, R. J.; Atkinson, M. J.; Monismith, S. G.; Schar, D. W. Continuous measurements of net production over a shallow reef community using a modified Eulerian approach. *J. Geophys. Res.* **2008**, *113*, C07035.
(14) Takeshita, Y.; McGillis, W.; Briggs, E. M.; Carter, A. L.; Donham, E. M.; Martz, T. R.; Price, N. N.; Smith, J. E. Assessment of net community production and calcification of a coral reef using a boundary layer approach. *J. Geophys. Res.: Oceans* **2016**, *121*, 5655−5671.
(15) Cullison Gray, S. E.; DeGrandpre, M. D.; Moore, T. S.; Martz, T. R.; Friederich, G. E.; Johnson, K. S. Applications of in situ pH measurements for inorganic carbon calculations. *Mar. Chem.* **2011**, *125*, 82−90.
(16) Dickson, A. G.; Afghan, J. D.; Anderson, G. C. Reference materials for oceanic CO2 analysis: a method for the certification of total alkalinity. *Mar. Chem.* **2003**, *80*, 185−197.
(17) Afshar, M. G.; Crespo, G. A.; Xie, X.; Bakker, E. Direct alkalinity detection with ion-selective chronopotentiometry. *Anal. Chem.* **2014**, *86*, 6461−6470.
(18) Afshar, M. G.; Crespo, G. A.; Bakker, E. Thin-Layer Chemical Modulations by a Combined Selective Proton Pump and pH Probe for Direct Alkalinity Detection. *Angew. Chem.* **2015**, *127*, 8228−8231.
(19) Afshar, M. G.; Tercier-Waeber, M.-L.; Wehrli, B.; Bakker, E. Direct sensing of total alkalinity profile in a stratified lake. *Geochem. Perspect. Lett.* **2017**, *3*, 85−93.
(20) Li, Q.; Wang, F.; Wang, Z. A.; Yuan, D.; Dai, M.; Chen, J.; Dai, J.; Hoering, K. A. Automated Spectrophotometric Analyzer for Rapid Single-Point Titration of Seawater Total Alkalinity. *Environ. Sci. Technol.* **2013**, *47*, 11139−11146.
(21) Martz, T. R.; Dickson, A. G.; DeGrandpre, M. D. Tracer Monitored Titrations: Measurement of Total Alkalinity. *Anal. Chem.* **2006**, *78*, 1817−1826.
(22) Spaulding, R. S.; DeGrandpre, M. D.; Beck, J. C.; Hart, R. D.; Peterson, B.; De Carlo, E. H.; Drupp, P. S.; Hammar, T. R. Autonomous in Situ Measurements of Seawater Alkalinity. *Environ. Sci. Technol.* **2014**, *48*, 9573.
(23) Briggs, E. M.; Sandoval, S.; Erten, A.; Takeshita, Y.; Kummel, A. C.; Martz, T. R. Solid State Sensor for Simultaneous Measurement of Total Alkalinity and pH of Seawater. *ACS Sens.* **2017**, *2*, 1302−1309.
(24) Johnson, K. S.; Jannasch, H. W.; Coletti, L. J.; Elrod, V. A.; Martz, T. R.; Takeshita, Y.; Carlson, R. J.; Connery, J. G. Deep-Sea DuraFET: A Pressure Tolerant pH Sensor Designed for Global Sensor Networks. *Anal. Chem.* **2016**, *88*, 3249−3256.
(25) Hofmann, G. E.; Smith, J. E.; Johnson, K. S.; Send, U.; Levin, L. A.; Micheli, F.; Paytan, A.; Price, N. N.; Peterson, B.; Takeshita, Y.; Matson, P. G.; Crook, E. D.; Kroeker, K. J.; Gambi, M. C.; Rivest, E. B.; Frieder, C. A.; Yu, P. C.; Martz, T. R. High-frequency dynamics of ocean pH: a multi-ecosystem comparison. *PLoS One* **2011**, *6*, No. e28983.
(26) Bresnahan, P. J., Jr.; Martz, T. R.; Takeshita, Y.; Johnson, K. S.; LaShomb, M. Best practices for autonomous measurement of seawater pH with the Honeywell Durafet. *Methods Oceanogr.* **2014**, *9*, 44−60.
(27) Eyre, B. D.; Andersson, A. J.; Cyronak, T. Benthic coral reef calcium carbonate dissolution in an acidifying ocean. *Nat. Clim. Change* **2014**, *4*, 969.
(28) Bates, N. R.; Michaels, A. F.; Knap, A. H. Alkalinity changes in the Sargasso Sea: geochemical evidence of calcification? *Mar. Chem.* **1996**, *51*, 347−358.
(29) Cross, J. N.; Mathis, J. T.; Bates, N. R.; Byrne, R. H. Conservative and non-conservative variations of total alkalinity on the southeastern Bering Sea shelf. *Mar. Chem.* **2013**, *154*, 100−112.
(30) Millero, F. J.; Lee, K.; Roche, M. Distribution of alkalinity in the surface waters of the major oceans. *Mar. Chem.* **1998**, *60*, 111−130.
(31) Martz, T. R.; Connery, J. G.; Johnson, K. S. Testing the Honeywell Durafet for seawater pH applications. *Limnol. Oceanogr.: Methods* **2010**, *8*, 172−184.
(32) Olthuis, W.; Luo, J.; Van der Schoot, B. H.; Bergveld, P.; Bos, M.; Van der Linden, W. E. Modelling of non-steady-state concentration profiles at ISFET-based coulometric sensor—actuator systems. *Anal. Chim. Acta* **1990**, *229*, 71−81.
(33) Connery, J. G.; Shaffer, E. W. Instrument for Potentiometric Electrochemical Measurements. U.S. Patent 4,851,104 A, July 25, 1989.
(34) Sutton, A. J.; Sabine, C. L.; Maenner-Jones, S.; Lawrence-Slavas, N.; Meinig, C.; Feely, R. A.; Mathis, J. T.; Musielewicz, S.; Bott, R.; McLain, P. D.; Fought, H. J.; Kozyr, A. A high-frequency atmospheric and seawater pCO_2 data set from 14 open-ocean sites using a moored autonomous system. *Earth Syst. Sci. Data* **2014**, *6*, 353−366.
(35) Hunter, C. L.; Evans, C. W. Coral reefs in Kaneohe Bay, Hawaii: two centuries of western influence and two decades of data. *Bull. Mar. Sci.* **1995**, *57*, 501−515.
(36) Lowe, R. J.; Falter, J. L.; Monismith, S. G.; Atkinson, M. J. Wave-Driven Circulation of a Coastal Reef−Lagoon System. *J. Phys. Oceanogr.* **2009**, *39*, 873−893.
(37) Lowe, R. J.; Falter, J. L.; Monismith, S. G.; Atkinson, M. J. A numerical study of circulation in a coastal reef-lagoon system. *J. Geophys. Res.* **2009**, *114*, C06022.
(38) Ho, D. T.; De Carlo, E. H.; Schlosser, P. Air-Sea Gas Exchange and CO_2 Fluxes in a Tropical Coral Reef Lagoon. *J. Geophys. Res.: Oceans* **2018**, *123*, 8701−8713.
(39) Fassbender, A. J.; Sabine, C. L.; Lawrence-Slavas, N.; De Carlo, E. H.; Meinig, C.; Maenner Jones, S. Robust Sensor for Extended Autonomous Measurements of Surface Ocean Dissolved Inorganic Carbon. *Environ. Sci. Technol.* **2015**, *49*, 3628−3635.
(40) Tamburri, M. ACT: Supporting Innovation for Better Ocean Prediction and Management. *Sea Technol.* **2011**, *52*, 29−30.
(41) Drupp, P. S.; De Carlo, E. H.; Mackenzie, F. T. Porewater CO_2−carbonic acid system chemistry in permeable carbonate reef sands. *Mar. Chem.* **2016**, *185*, 48−64.
(42) Eyre, B. D.; Cyronak, T.; Drupp, P.; De Carlo, E. H.; Sachs, J. P.; Andersson, A. J. Coral reefs will transition to net dissolving before end of century. *Science* **2018**, *359*, 908−911.
(43) Dickson, A. G.; Sabine, C. L.; Christian, J. R. *Guide to Best Practices for Ocean CO_2 Measurements*; North Pacific Marine Science Organization, 2007.
(44) Johnson, K. S.; Plant, J. N.; Coletti, L. J.; Jannasch, H. W.; Sakamoto, C. M.; Riser, S. C.; Swift, D. D.; Williams, N. L.; Boss, E.;

Haëntjens, N.; Talley, L. D.; Sarmiento, J. L. Biogeochemical sensor performance in the SOCCOM profiling float array. *J. Geophys. Res.: Oceans* **2017**, *122*, 6416−6436.
(45) Pierrot, D.; Lewis, E.; Wallace, D. CO2SYS DOS Program developed for CO_2 system calculations. *ORNL/CDIAC-105*; Carbon Dioxide Information Analysis Center, Oak Ridge National Laboratory, US Department of Energy: Oak Ridge, TN, 2006.
(46) Terlouw, G. J.; Knor, L.; De Carlo, E. H.; Drupp, P. S.; Mackenzie, F. T.; Li, Y.-H.; Sutton, A. J.; Pleuddemann, A.; Sabine, C. L. Hawaii Coastal MApCO_2 Network: A statistical evaluation of eight years of observations on tropical coral reefs. *Front. Mar. Sci.* **2019**, *6*, 226.
(47) Kealoha, A. K.; Shamberger, K. E. F.; Reid, E. C.; Davis, K. A.; Lentz, S. J.; Brainard, R. E.; Oliver, T. A.; Rappé, M. S.; Roark, E. B.; Rii, Y. M. Heterotrophy of Oceanic Particulate Organic Matter Elevates Net Ecosystem Calcification. *Geophys. Res. Lett.* **2019**, *46*, 9851−9860.

https://dx.doi.org/10.1021/acsearthspacechem.9b00274
ACS Earth Space Chem. 2020, 4, 355−362